

1 **Gnotobiotic zebrafish microbiota display inter-individual**  
2 **variability affecting host physiology**

3

4 Emmanuel E. Adade<sup>1,2,\*</sup>, Rebecca J. Stevick<sup>3,\*</sup>, David Pérez-Pascual<sup>3</sup>, Jean-Marc Ghigo<sup>3#</sup>,  
5 Alex M. Valm<sup>1,2#</sup>

6

7 <sup>1</sup>Department of Biological Sciences, State University of New York at Albany, Albany, NY  
8 12222, USA

9 <sup>2</sup>The RNA Institute, State University of New York at Albany, Albany, NY 12222, USA

10 <sup>3</sup>Institut Pasteur, Université de Paris Cité, CNRS UMR 6047, Genetics of Biofilms

11 Laboratory, Paris F-75015, France

12

13 \*These authors contributed equally to this work.

14

15 # Co-corresponding Authors: Jean-Marc Ghigo, [jmghigo@pasteur.fr](mailto:jmghigo@pasteur.fr); Alex Valm,

16 [avalm@albany.edu](mailto:avalm@albany.edu)

17

18 **Competing Interests:** The authors declare no competing financial interests.

19

20 **Keywords:** Zebrafish; gnotobiotic model; microbiota; phenotypic variability; FISH; Mucus

21

## 22 **Abstract**

23

24 Gnotobiotic animal models reconventionalized under controlled laboratory conditions with  
25 multi-species bacterial communities are commonly used to study host-microbiota interactions  
26 under presumably more reproducible conditions than conventional animals. The usefulness of  
27 these models is however limited by inter-animal variability in bacterial colonization and our  
28 general lack of understanding of the inter-individual fluctuation and spatio-temporal dynamics  
29 of microbiota assemblies at the micron to millimeter scale. Here, we show underreported  
30 variability in gnotobiotic models by analyzing differences in gut colonization efficiency,  
31 bacterial composition, and host intestinal mucus production between conventional and  
32 gnotobiotic zebrafish larvae re-conventionalized with a mix of 9 bacteria isolated from  
33 conventional microbiota. Despite similar bacterial community composition, we observed high  
34 variability in the spatial distribution of bacteria along the intestinal tract in the  
35 reconventionalized model. We also observed that, whereas bacteria abundance and intestinal  
36 mucus per fish were not correlated, reconventionalized fish had lower intestinal mucus  
37 compared to conventional animals, indicating that the stimulation of mucus production depends  
38 on the microbiota composition. Our findings, therefore, suggest that variable colonization  
39 phenotypes affect host physiology and impact the reproducibility of experimental outcomes in  
40 studies that use gnotobiotic animals. This work provides insights into the heterogeneity of  
41 gnotobiotic models and the need to accurately assess re-conventionalization for reproducibility  
42 in host-microbiota studies.

43

## 44 **Introduction**

45 Host-associated microbiota play essential roles in host physiology and health (1). Numerous  
46 studies have explored the perturbation of this microbiota in order to understand its contribution  
47 to host function, particularly for disease resistance, antibiotic effects, gut health, environmental  
48 factors, and many others (2–5). However, the complexity and heterogeneity of conventional  
49 host-associated microbiota, containing unculturable microorganisms and unknown functions,  
50 in humans and animal models limits mechanistic understanding.

51  
52 In contrast to conventional animals with relatively complex microbiota (6), axenic (germ-free)  
53 and gnotobiotic animal models are powerful tools to study microbial contributions to host  
54 functions. These models allow for direct manipulation of bacterial genetics, composition, and  
55 exposure to determine the key drivers of microbiota-associated phenotypes under presumably  
56 more reproducible conditions. However, despite the capacity to control many aspects of  
57 gnotobiotic models, the inherent heterogeneity in biological systems could still contribute to  
58 phenotypic variability. In the context of host-associated microbiota, this could be due to pooled  
59 tissue samples, averaged replication, pseudo-replication within treatment conditions, and/or the  
60 use of simplified core microbiota (7,8). For example, previous studies of gnotobiotic mice have  
61 explored inter-facility microbiota variability (9) or colonization over time (10), but the samples  
62 were pooled prior to analysis and only presence/absence of taxa per group was considered.

63  
64 Similarly, the study of host-pathogen-microbiota interactions in gnotobiotic zebrafish, an  
65 emerging model recapitulating many salient features of the mammalian gastrointestinal tract  
66 (11,12), is also subjected to variability. We indeed previously showed that  
67 reconventionalization of axenic zebrafish with bacterial strains isolated from the conventional  
68 fish provides variable protection against the fish pathogen *Flavobacterium columnare* (13).  
69 This suggests that gnotobiotic zebrafish reproducibly reconventionalized with a controlled  
70 bacterial consortium is prone to underreported inter-individual variability that may be the origin  
71 of phenotypic variation.

72  
73 Here we explored this issue by investigating intra and inter-individual microbial composition,  
74 colonization biogeography and host mucus production as an indicator of host physiology in  
75 conventional and gnotobiotic zebrafish models. We generated gnotobiotic animals using a  
76 previously-studied consortium of 9 bacterial strains isolated from the conventional fish

77 microbiota (13). We showed that larval zebrafish gut bacterial load fluctuates and that bacterial  
78 colonization, composition and biogeography varies between conventional and gnotobiotic fish  
79 models, which impacts zebrafish mucus production and tissue architecture. While providing  
80 insights on baseline variability of gnotobiotic models harboring bacterial communities of  
81 reduced complexity under control conditions, our study also illustrates the necessity to  
82 characterize this variability before investigating the effects of antibiotics, disease, or other  
83 perturbations on host-associated microbiota.  
84

## 85 Results

### 86 Bacterial colonization of zebrafish larvae fluctuates and is localized to the gut

87 In order to investigate inherent variability between conventional zebrafish and zebrafish  
88 reconventionalized with the previously-studied consortium of 9 bacterial strains (Mix9) isolated  
89 from the conventional fish microbiota (13), we measured the bacterial biovolume in zebrafish  
90 tagged with the universal bacterial probe Eub338 (14) (**Fig 1A-D**). We observed significantly  
91 higher bacterial colonization in the conventional larvae than in the Mix9 fish, with median  
92 bacteria biovolume of  $2.7 \times 10^5 \mu\text{m}^3$  and  $2.6 \times 10^4 \mu\text{m}^3$  respectively (p-value = 0.035) (**Fig 1E**).  
93 These bacterial biomasses were primarily localized to the intestinal region of the larval  
94 zebrafish, with a smaller number of cells colonizing the skin (**Fig 1A-D**). Consistent with  
95 sterility tests performed throughout the study, no bacteria were detected in axenic (germ-free)  
96 zebrafish (**Fig 1E**). We then analyzed a larger sample of 24 reconventionalized Mix9 larvae,  
97 and we observed a high variability in bacterial biovolume among experimental animals as  
98 measured with confocal imaging (**Fig S1**). CFU counting corresponding to entire homogenized  
99 zebrafish plated on agar growth medium confirmed the variability observed in the FISH  
100 biovolume measurements (**Fig 1F**).  
101

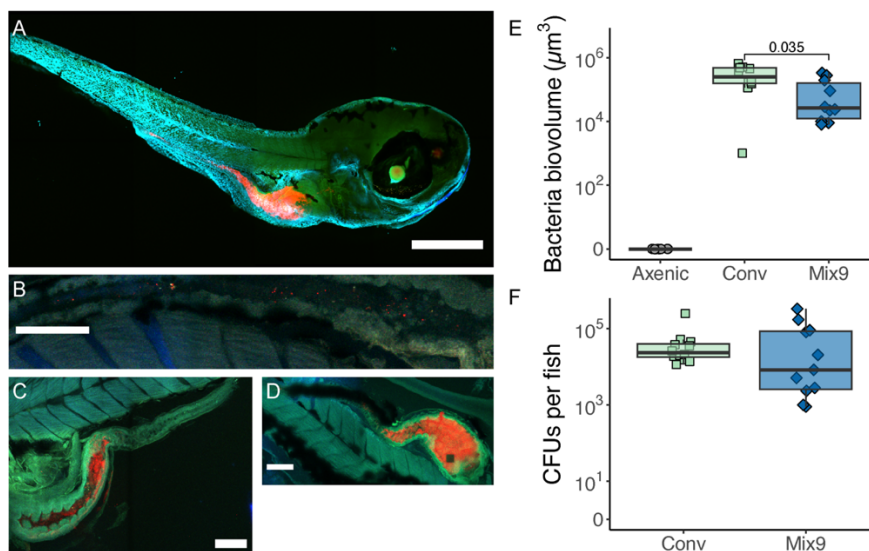


**Figure 1. Bacterial load was localized in the larval zebrafish gut and showed colonization variability.** (A) Detection of bacteria by Fluorescent in situ Hybridization (FISH) on fixed zebrafish larvae exposed to Mix9 at 7 days post fertilization (dpf) showed the bacteria localized primarily in the gut. Representative images of (B) zebrafish gut with low bacterial load, (C) zebrafish gut with medium bacterial load, and (D) zebrafish gut with high bacterial load. (A-D) EUB 338 conjugated with Alexa Fluor 594 (Red)– All bacteria, DAPI (Blue) – (host nuclei), Zebrafish autofluorescence in (Green). Scale bars (A) = 200  $\mu\text{m}$ , (B, D) = 100  $\mu\text{m}$  and (C) = 40  $\mu\text{m}$ . (E) Bacterial biovolume as a measure of abundance with FISH. Unpaired T- test (alpha = 0.05) was used to measure significance in variation between conventional and Mix9 (n = 10). (F) Quantification of bacterial load in whole larval zebrafish (Conventional and Mix 9) via culturable CFUs. Bacterial load quantification via CFU counts of homogenized Mix9 fish on LB media at 7 dpf (n = 10). Note log scale on y-axis for (E) and (F).

102 **Bacterial colonization biogeography varies between conventional and gnotobiotic**  
103 **models**

104 In addition to the bacterial load, we also examined the bacterial biogeography per fish and  
105 observed that there is variability in the bacterial localization along the length of the intestinal  
106 tract (**Fig 2A**) in both conventional and gnotobiotic Mix9 zebrafish larval models (**Fig 2B**).  
107 Conventional larvae were characterized by a consistently high bacterial load in the bulb and  
108 less in the proximal intestine and on average lower but heterogeneous bacterial load in the distal  
109 intestine (**Fig 2D**). However, Mix9 larvae had a highly heterogeneous bacterial load in the bulb  
110 among animals ranging from no bacteria to approximately  $1 \times 10^5 \mu\text{m}^3$  of bacteria, and more  
111 consistent biovolumes in the proximal and distal intestines (**Fig 2E**).

112

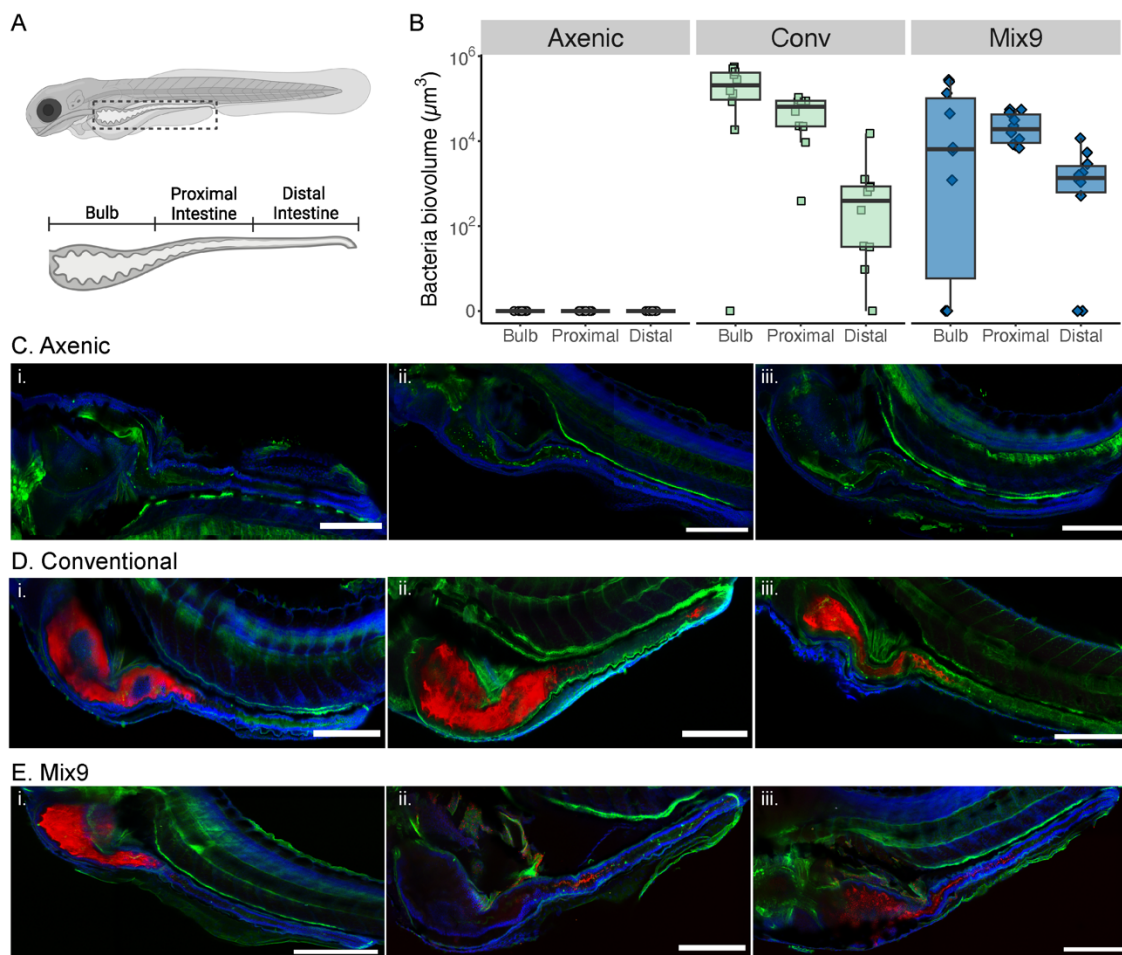


**Figure 2. Bacterial biogeography and abundance along the gastrointestinal tracts of the larval zebrafish.** (A) A schematic of the larval stage zebrafish with the gut highlighted. [Inset] The schematic gut of the larval zebrafish with the segmentation classifying the three sections of the gut analyzed here. (B) Analysis of the spatial distribution of bacteria in the gut for the various conditions (n=10). (C – E) Confocal images of representative larvae in each condition shown. i, ii and iii show three representative images for each condition. Universal bacteria probe EUB 338 conjugated with Alexa Fluor 594 (Red)– All bacteria, DAPI (Blue) – host nuclei, WGA conjugated with Oregon Green 488 (Green) – Mucus in the fish. All scale bars = 200  $\mu\text{m}$ .

### 113 **Microbiota in conventional zebrafish larvae is more diverse than in gnotobiotic larvae**

114 We further evaluated the differences in bacterial composition between conventional and  
115 gnotobiotic zebrafish using 16S rRNA gene amplicon sequencing (**Fig S2**). Despite the reduced  
116 community administered to the gnotobiotic Mix9 zebrafish, their composition at the phylum  
117 level is not significantly different from the conventional fish (**Fig 3A**). Both the conventional  
118 and Mix9 fish bacterial composition is dominated by > 90 % Proteobacteria, with the remainder  
119 in the Bacteroidota and Actinobacteria phyla. At the Amplicon Sequence Variant (ASV) level,  
120 the conventional fish microbiome is mainly comprised of a single *Aeromonas* sp. ASV 02, with  
121 over 50 % relative abundance in each sample (**Fig 3B**). There was a relative decrease in  
122 *Aeromonas* sp. ASV 02 and an increase in ASV 01 unclassified Gammaproteobacteria (likely  
123 *Pseudomonas* sp.) in the Mix9 condition, compared to conventional fish (**Fig 3B**). Despite  
124 addition of 9 bacterial strains in equal proportion to the axenic fish model at 4 dpf, only two  
125 ASVs were identified in all fish at 7 dpf: 02 *Aeromonas* sp. and 01 Gammaproteobacteria  
126 *Pseudomonas* sp. These two ASVs may comprise multiple strains of the Mix9 that are  
127 indistinguishable at the 16S rRNA level.

128  
129 Conventional and Mix9 fish shared 32 ASVs, while conventional fish had 54 unique ASVs  
130 (55% of total ASVs) (**Fig 4A**). Despite many shared taxa, the conventional fish microbiota had  
131 a significantly higher alpha-diversity than the Mix9 fish microbiota as measured by Chao and  
132 Shannon indices, but not Simpsons index (**Fig 4B**). Simpson's index has decreased sensitivity  
133 to less abundant taxa, indicating that the differences between the two models is in the rare taxa  
134 and that the most abundant taxa are comparable. This is further demonstrated with no significant  
135 difference in beta-diversity or beta-dispersion between the conventional and Mix9 microbiota  
136 (**Fig 4C-D**). Overall, the conventional fish have a higher richness and increased number of less  
137 abundant taxa than the simplified microbiota introduced in the Mix9 gnotobiotic fish.

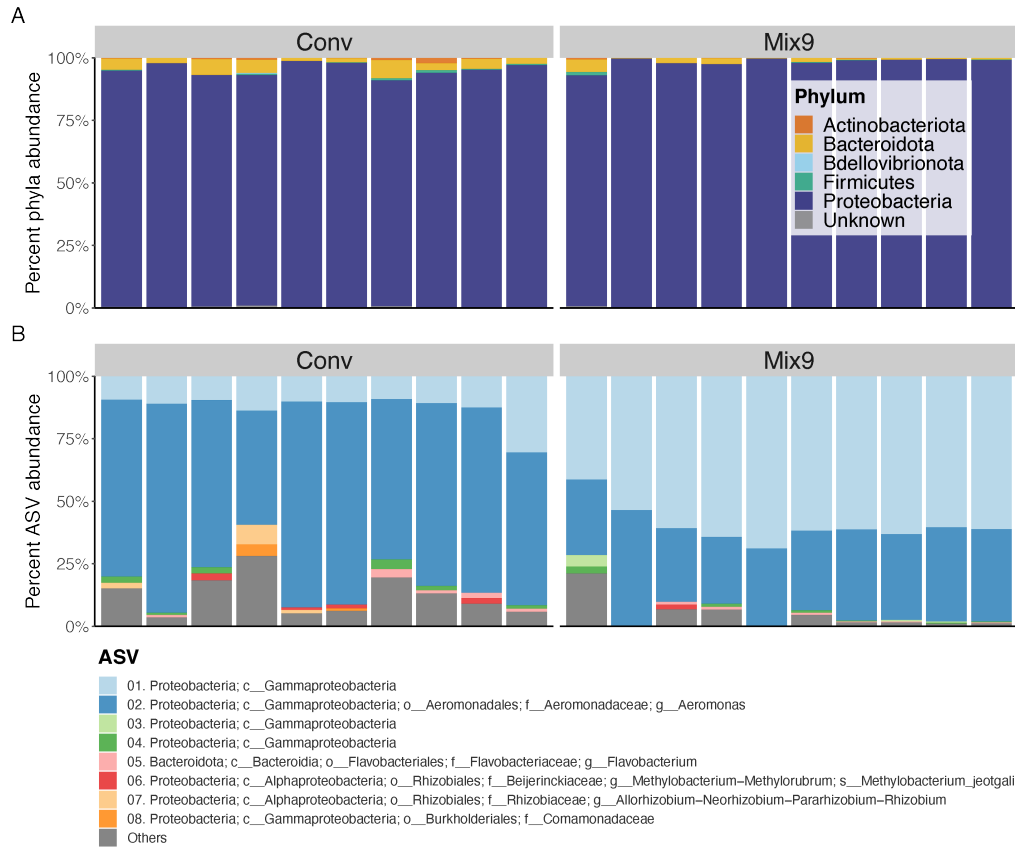


**Figure 3. Bacterial composition of conventional and Mix9 fish at the (A) Phylum and (B) ASV level.** Each stacked bar represents an individual larval fish sampled at 7 dpf with  $n = 10$  individual fish per condition. **(A)** Bar plots of percent phylum abundance per sample. **(B)** Bar plots of percent Amplicon Sequence Variant (ASV) abundance per sample. The top 8 most abundant ASVs are shown with the others grouped into “Others.”

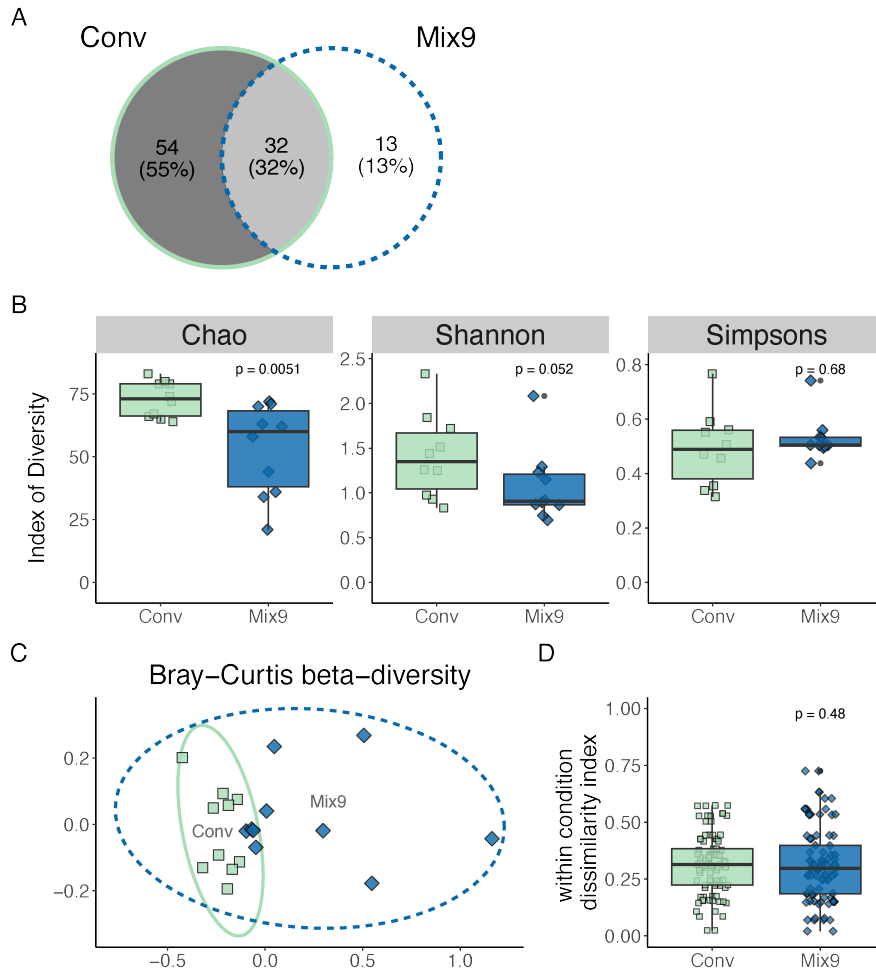


**Figure 4. Alpha- and beta-diversity of individual conventional and Mix9 fish bacterial communities measured using 16S rRNA amplicons. (A)** Venn diagram of ASVs shared between conventional (Conv) and Mix9 conditions. All ASVs with less than 5 reads were removed. **(B)** Alpha-diversity calculated using Chao richness, Shannon, and Simpson's indices. **(C)** NMDS plot calculated using Bray-Curtis beta-diversity ( $k=2$ ) of percent normalized ASVs for conventional and Mix9 samples. Ellipse lines show the 95 % confidence interval (standard deviation). Stress = 0.055. **(D)** Beta-dispersion or within-condition dissimilarity index calculated using Bray-Curtis beta-diversity. **For all panels:**  $n = 10$ , Wilcoxon test for Mix9 compared to the Conventional (Conv) condition.

139

## 140 **Changes in zebrafish mucus production and tissue architecture depend on microbiota** 141 **composition and colonization**

142 Mucus, composed mostly of the highly O-glycosylated mucins, coats the epithelial surfaces of  
143 the gastrointestinal tract and has important functions, including the prevention of colonization  
144 by foreign microbes (15–20). The interactions among resident gut microbes and between  
145 microbiota and host has been shown to influence mucus production and shape microbiota  
146 spatial distribution on a macroscale (21). To better understand mucus biogeography and its  
147 potential variability, we monitored the presence of gut mucus in the conventional, axenic and  
148 Mix9 zebrafish models with fluorescent wheat germ agglutinin (WGA) staining (**Fig 5A-D**).

149 Intriguingly, we observed little correlation between total bacterial load and mucus abundance,  
150 per animal, in the conventional and Mix9 models (**Fig 5E-F**). This suggests that induction of  
151 mucus production by the gut microbiome may be more dependent upon the presence and  
152 distribution of specific organisms, rather than the total bacterial biomass. Comparison of mucus  
153 levels in all 3 models focused on the intestine only, because the bulb tissue architecture was  
154 degenerated in the axenic control, and therefore difficult to quantify with imaging. We observed  
155 that mucus abundance was highest in conventional fish, intermediate in Mix9 and lowest in  
156 axenic (**Fig 5G-H**). Histological staining with Alcian blue and Periodic-Acid Schiff (PAS)  
157 stains performed at 7 dpf (72 h post-reconventionalization) on axenic, conventional, and Mix9  
158 gnotobiotic larvae did not show any major qualitative difference in their intestinal organization  
159 (**Fig S3**).

160

161 Together these data suggest that bacterial colonization and composition affect mucus  
162 production without any impact on the tissue architecture, leading to changes in host physiology,  
163 with the highest variability in the Mix9 gnotobiotic condition.

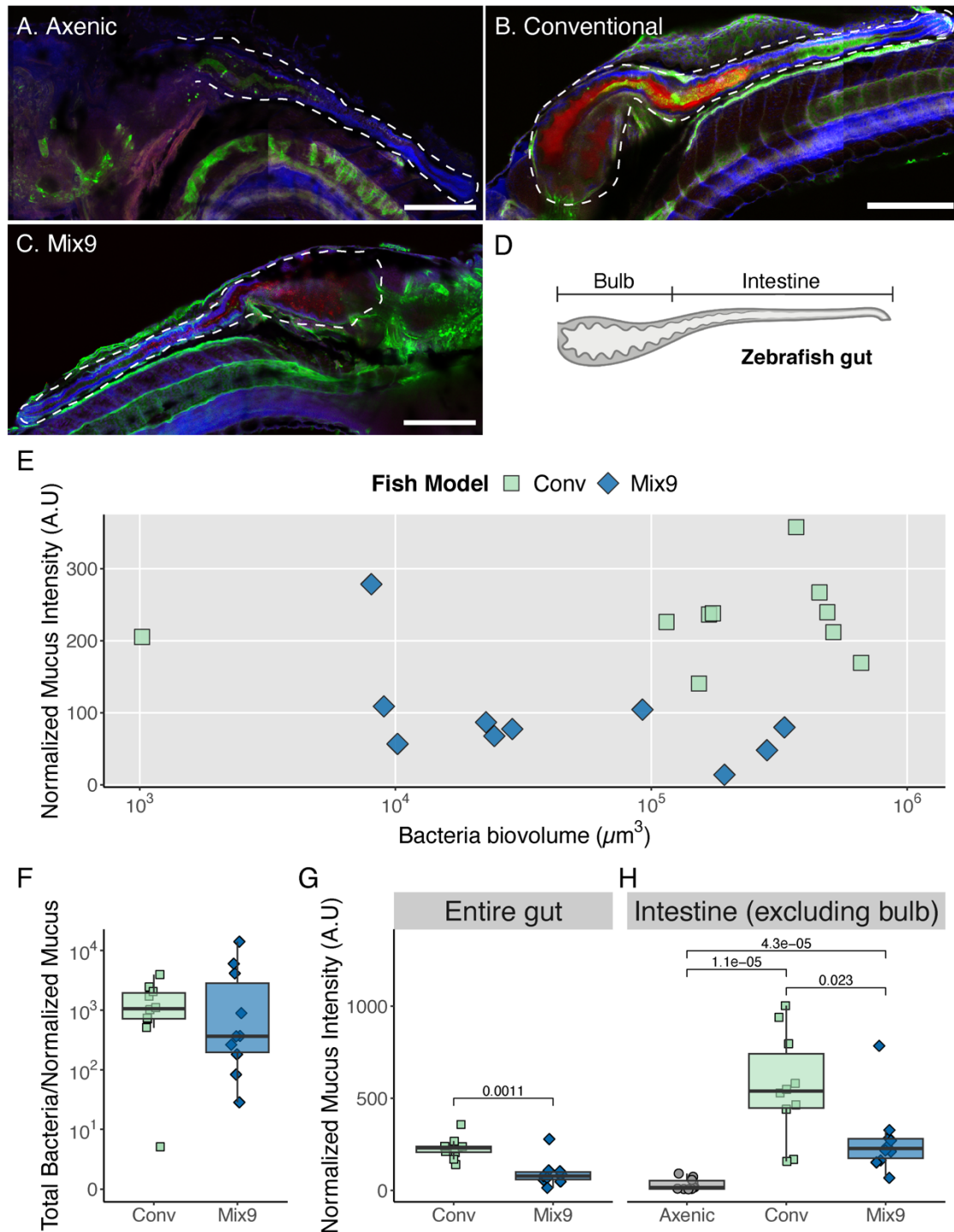


**Figure 5. Zebrafish intestinal mucus production in multi-member gnotobiotic model is different than conventional fish.** (A – C) Confocal images of the gut region of the zebrafish for each condition. Universal bacteria probe EUB 338 conjugated with Alexa Fluor 594 (Red) – All bacteria, DAPI (Blue) – (host nuclei), WGA conjugated with Oregon Green 488 (Green) – Mucus in the fish, (Magenta) – Zebrafish autofluorescence. All scale bars = 200  $\mu\text{m}$ . (D) The schematic larval zebrafish gut with the segmentation classifying the two sections of the gut analyzed here. (E) Per fish correlation of total bacteria load and normalized mucus intensities. (F) The relative measurement of mucus to bacteria biovolume per fish shown on a log scale. (G-H) Normalized mucus intensity in the entire gut and intestine excluding bulb. For entire gut, T-tests were used to estimate the statistical significance ( $\alpha = 0.05$ ),  $p$ -values  $< 0.05$  were significant. For intestine only, One-Way ANOVA and Tukey post hoc test was used to statistically measure the variation among the various conditions,  $p$ -values  $< 0.05$  were significant. ( $n = 10$ ).

## 165 **Discussion**

166 In this study, we explored the inter-individual relationship between host bacterial colonization,  
167 composition, and mucus production as an indicator of host physiology. Whereas the  
168 conventional zebrafish showed higher taxonomic diversity than the Mix9 gnotobiotic zebrafish,  
169 their microbiota beta-diversity was not significantly different. Nevertheless, our analysis  
170 revealed a remarkable heterogeneity in the distribution of bacteria along the length of the gut  
171 in the gnotobiotic model. Heterogeneity in the biogeography and abundance of bacteria along  
172 the longitudinal (mouth to anus) and transverse (epithelium to lumen) axes of the gut is known  
173 to be driven by numerous host, microbial and environmental factors. This includes peristaltic  
174 activity, microbial motility, mucus architecture, chemical and nutrient gradients, host immunity  
175 and both synergistic and antagonistic bacterial interactions (22,16,23–26). Intriguingly, we  
176 observed bacteria as individual cells, small aggregates, and large clusters in the gut in our Mix9  
177 gnotobiotic model.

178  
179 As previously reported, mucus was generally more abundant in the bulb and proximal region  
180 of the zebrafish gut (20), but its overall abundance was highest in conventional larvae,  
181 intermediate in Mix 9 and lowest in axenic larvae. Similar observations were made in axenic  
182 (germ-free) mice, in which mucus was shown to differ in the small and large intestine, and to  
183 depend on their bacterial composition (27–29). These results are therefore indicative of a  
184 dynamic interrelationship between microbiota and host mucus production that is not only due  
185 to the presence or absence of a microbiota but results more from subtle spatial relationships  
186 between specific microbial taxa and the host. We hypothesize that there may be different  
187 combinations of bacteria species locally present in each fish gut in a spatially dependent  
188 manner. Further analysis of gut biogeography and architecture with higher phylogenetic  
189 resolution may provide support for this hypothesis.

190  
191 The reduced complexity of our gnotobiotic zebrafish model enabled us to observe that the Mix9  
192 bacterial consortium restored bulb tissue architecture, including mucus production, that  
193 otherwise deteriorated in axenic animals. Interestingly, our histological analysis showed that  
194 the gut tissue of axenic and Mix9 fish appeared morphologically no different to conventional  
195 ones, consistent with previously reported phenotypic analysis of gnotobiotic zebrafish (30,31).  
196 These studies also reported a significant decrease in the number of Goblet cells in axenic  
197 zebrafish larvae compared to conventional ones (30). These discrepancies could originate from

198 the different feeding protocols and the use of sterile powder food versus sterile live *T.*  
199 *thermophila* in our study (31) or even not fed at all (30).

200

201 Despite the use of autochthonous bacterial strains isolated from conventional zebrafish larvae,  
202 we observed a high variability in bacterial load as well as in microbiota and spatial structure in  
203 gnotobiotic Mix9 larvae compared to conventional fish. Whereas this was previously observed  
204 in zebrafish larvae mono-reconventionalized with *Pseudomonas* sp. or *Aeromonas* sp., strains  
205 (30), our data identified an important limitation as gnotobiotic animals reconventionalized with  
206 low complexity microbiomes exhibit heterogeneous colonization efficiencies and mucus  
207 phenotypes not observed in conventional animals, which may have profound implications for  
208 reproducibility.

209

210 Various phenomena could affect the assembly of the microbiota in our gnotobiotic model,  
211 including differences in bacterial migration into the fish, survival to the gut environment,  
212 bacterial interactions, intestinal expulsion, or predation by live *Tetrahymena* used as zebrafish  
213 food source (32). In addition, the administration of bacteria in fish water and their acquisition  
214 by natural routes may contribute to the observed variability in colonization (12). The use of  
215 direct and more controlled inoculation methods including microinjection or gavage could  
216 reduce colonization heterogeneity.

217

218 Gnotobiotic animal models are invaluable tools to study host-associated microbiota function.  
219 However, our study demonstrates that special attention should be given to key parameters such  
220 as bacterial load and composition before assuming control and reproducibility of the results  
221 obtained with these gnotobiotic models (33). These criteria should be taken into consideration  
222 as they are likely to impact colonization efficiency as well as effects on the host and future  
223 studies of the factors stabilizing host-microbiota interactions will contribute to validate and  
224 increase the usefulness of gnotobiotic approaches.

225

## 226 **Methods**

### 227 **General zebrafish husbandry**

228 Wild-type AB/AB zebrafish (*Danio rerio*) fertilized eggs at 0 days post fertilization (dpf) were  
229 obtained from the Zorngl'hub platform at Institut Pasteur. All procedures were performed at  
230 28°C under a laminar microbiological hood with single-use plastic ware according to European  
231 Union guidelines for handling of laboratory animals and were approved by the relevant  
232 institutional Animal Health and Care Committees. Eggs were kept in 25 cm<sup>3</sup> vented flasks  
233 (Corning 430639) with 20 mL of autoclaved mineral water (Volvic) until 4 dpf (30 – 33  
234 eggs/flask), transferred to new flasks after hatching at 4 dpf (10 – 15 fish/flask), then transferred  
235 to individual wells of a 24-well plate (TPP 92024) at 6 dpf. At the end of the experiment,  
236 zebrafish were euthanized with tricaine (MS-222, Sigma-Aldrich E10521) at 0.3 mg/mL. Fish  
237 were fed with sterile *T. thermophila* every 48 hours starting at 4 dpf as previously described  
238 (34).

239

### 240 **Zebrafish sterilization and reconventionalization**

241 The zebrafish embryos were sterilized as previously described at 1 dpf and then maintained as  
242 described above (13). Sterility was confirmed at 3 dpf by spotting 50 µL of water from each  
243 flask on LB, TYES and YPD agar plates and incubated at 28 °C under aerobic conditions for at  
244 least 3 days. Contaminated flasks were immediately removed from the experiment and not  
245 included in the results. Axenic zebrafish larvae were reconventionalized at 4 dpf, as follows.  
246 Overnight cultures of a single bacterial colony in 5 mL of liquid media were washed twice with  
247 sterile mineral water (Volvic) and normalized to OD-0.1 in water. For Mix9  
248 reconventionalization, 200 µL of each strain was added per flask at a final concentration of 5 x  
249 10<sup>5</sup> CFU/mL per strain. Water samples were plated in serial dilutions to confirm final bacterial  
250 concentration and sterility. Reconventionalization was performed for 48 hours until fish were  
251 transferred to sterile water in 24-well plates at 6 dpf.

252

### 253 **Bacterial strains and growth conditions**

254 Bacterial strains are listed in Table 1. All strains were grown in Miller's Lysogeny Broth (LB)  
255 (Corning) and incubated at 28°C with rotation. Cultures on solid media were on LB with 1.5 %  
256 agar. Bacteria were always streaked from glycerol stocks stored at -80°C on LB- agar before

257 inoculation with a single colony in liquid cultures. All media and chemicals were purchased  
258 from Sigma-Aldrich.

259

260 **Table 1. Bacterial strains used in this study.** All strains were isolated from conventional  
261 zebrafish larvae (13).

Code	Strain
UGB3608	<i>Aeromonas veronii 1</i>
UGB3612	<i>Pseudomonas mossellii</i>
UGB3616	<i>Stenotrophomas maltophilia</i>
UGB3607	<i>Aeromonas caviae</i>
UGB3614	<i>Pseudomonas peli</i>
UGB3615	<i>Pseudomonas sediminis</i>
UGB3611	<i>Phyllobacterium myrsinacearum</i>
UGB3609	<i>Aeromonas veronii 2</i>
UGB3613	<i>Pseudomonas nitroreducens</i>

262

### 263 **Quantification of zebrafish bacterial load via CFU counts**

264 Zebrafish were sampled at 7 dpf and washed twice by 2 transfers to clean, sterile water in petri  
265 dishes to remove loosely attached bacteria. The larvae were then added in 500  $\mu$ L of sterile  
266 water to 2 mL tubes containing 1.4 mm ceramic beads (Fischer Scientific 15555799) and  
267 homogenized for 2 x 45 seconds at 6000 rpm using a 24 Touch Homogenizer (Bertin  
268 Instruments). These homogenization conditions are sufficient to lyse zebrafish tissue, but not  
269 harmful to the bacteria. The lysate was then diluted from 10- 100-fold and 3 x 100  $\mu$ L from  
270 each dilution was spread on LB agar using sterile glass beads. After 2 days of incubation at  
271 28°C, CFUs were counted per fish and calculated by 500  $\mu$ L lysate / 100  $\mu$ L plated \* dilution  
272 factor \* (average of replicate CFUs).

273

### 274 **Zebrafish sampling and DNA extraction**

275 At 7 dpf, 10 zebrafish of each conventional and Mix9 conditions were sampled and washed  
276 twice by 2 transfers to clean, sterile water in petri dishes. Each fish was then added to a sterile  
277 2-mL microcentrifuge tube and euthanized with tricaine at 0.3 mg/mL. All liquid was removed  
278 from the tissue and the samples were immediately frozen at -80°C until DNA extraction. DNA  
279 extraction was performed from single larval zebrafish using the DNeasy Blood & Tissue kit

280 (Qiagen 69504) with modifications as follows. Tissue samples were thawed at room  
281 temperature, then 380  $\mu$ L Buffer ATL and 20  $\mu$ L proteinase K were added directly to each  
282 individual larva in a 2 mL tube. Samples were vortexed, then incubated overnight (15-18 hours)  
283 at 56°C and 300 rpm until fully lysed. After lysis, 4  $\mu$ L of RNase A solution was added and  
284 the samples were incubated for 5 minutes at room temperature to remove residual RNA. Next,  
285 400  $\mu$ L Buffer AL and 400  $\mu$ L 100 % ethanol were added and mixed by vortexing before  
286 loading the lysate onto the DNeasy mini spin column in 2 x 600  $\mu$ L loads. DNA purification  
287 and cleanup proceeded according to the manufacturer's recommendations with a final elution  
288 volume of 50  $\mu$ L in Buffer AE. Purified DNA was quantified using the Qubit HS DNA  
289 fluorometer kit (ThermoFisher Q32851) and purity was assessed with the Nanodrop  
290 spectrophotometer (ThermoFisher). Negative controls for the extraction kit were prepared  
291 alongside zebrafish samples, but with no tissue input.

292

### 293 **Zebrafish 16S rRNA amplicon sequencing and analysis**

294 16S rRNA gene amplicons of the V6 region for the 10 conventional zebrafish samples, 10 Mix9  
295 zebrafish samples, 2 mock community samples (Zymo Research DNA standard I D6305), 2  
296 negative DNA extraction samples, and blank PCR control were prepared using 967F/1064R  
297 primers. A two-step PCR reaction using 200 ng of zebrafish DNA was performed in duplicate  
298 50  $\mu$ L reactions as previously described (35,36). Each first step reaction included 25  $\mu$ L 2X  
299 Phusion Mastermix (Thermo Scientific F531S), 1.5  $\mu$ L of 10  $\mu$ M F/R primer mix, 13 - 20  $\mu$ L  
300 template DNA (200 ng), and 3.5 - 10.5  $\mu$ L nuclease-free water (up to 50  $\mu$ L). PCR  
301 amplification (step 1) conditions were denaturing at 98°C for 3 min followed by 30 cycles of  
302 denaturation at 98°C for 10 s, primer annealing at 56°C for 30 s, and extension at 72°C for 20  
303 s, then a final extension at 72°C for 20 s. Negative controls for the PCR reagents were prepared  
304 alongside zebrafish DNA samples, but with additional nuclease-free water input. PCR products  
305 were assessed for concentration (Qubit DNA HS reagents) and expected size using agarose gel  
306 electrophoresis. A second PCR step was performed to attach sequencing barcodes and adaptors  
307 according to Illumina protocols. The PCR products were analyzed with 250 bp paired-end  
308 sequencing to obtain overlapping reads on an Illumina MiSeq at the Institut Pasteur Biomics  
309 platform.

310

311 The resulting 16S rRNA gene amplicon sequences were demultiplexed and quality filtered  
312 using DADA2 (v1.6.0) implemented in QIIME2 (v2020.11.1) with additional parameters --p-

313 trunc-len-r 80 --p-trunc-len-f 80 --p-trim-left-r 19 --p-trim-left-f 19 to determine amplicon  
314 sequence variants (ASVs) (37,38). All ASVs were summarized with the QIIME2 pipeline  
315 (v2020.11.1) and classified directly using the SILVA database (99 % similarity, release #134)  
316 (39,40). Processed ASV and associated taxonomy data was exported as a count matrix for  
317 analysis in R (v4.1.3). The positive and negative controls were checked to ensure sequencing  
318 quality and expected relative abundances. Non-bacterial and chloroplast sequences were then  
319 removed, and the data was normalized by percentage to the total ASVs. All ASVs with less  
320 than 0.1% abundance were removed from each sample for further dissimilarity metric analysis  
321 (41).

322  
323 All descriptive and statistical analyses were performed in the R statistical computing  
324 environment with the *tidyverse* v1.3.1, *vegan* v2.5.7 and *phyloseq* v1.38.0 packages (42–44).  
325 Non-metric dimensional analysis (NMDS) was used to determine the influence of fish type on  
326 the ASV-level composition. The Bray-Curtis dissimilarity metric was calculated with  $k = 2$  for  
327 max 50 iterations and 95 % confidence intervals (standard deviation) were plotted. Statistical  
328 testing of the beta-diversity was done using the PERMANOVA *adonis2* test implemented in  
329 *vegan* (method = "bray",  $k = 2$ ) (45,46). Within-condition variability was calculated using the  
330 command `vegdist(method = "bray", k = 2)` and the matrix was simplified to include samples  
331 compared within each timepoint. Alpha-diversity metrics were calculated for each sample at  
332 the ASV level using the *vegan* package and analyzed using the non-parametric Kruskal–Wallis  
333 rank sum test in R. All processed sequencing files, bash scripts, QIIME2 artifacts, and Rmd  
334 scripts to reproduce the figures in the manuscript are available on Zenodo (47).

335

### 336 **Estimation of zebrafish bacterial load via FISH and mucus labelling**

337 Whole larval zebrafish reconventionalized with Mix9 were preserved with Carnoy's fixative  
338 24 hours after infection (72 hours after reconventionalization) and bacteria were labelled using  
339 the Eub338 general probe by fluorescent in situ hybridization (FISH). The fish samples were  
340 imaged using confocal fluorescent microscopy to localize and quantify the bacterial load in  
341 each fish. Labeling of zebrafish was carried out in Eppendorf tubes. Carnoy's fixed zebrafish  
342 samples were washed in PBS for 3 mins. For the bacteria labelling, to each tube, 200  $\mu$ l of  
343 hybridization buffer [0.09 M NaCl, 0.02 M Tris pH 7.5, 0.01 % SDS, 20 % formamide] and 2  
344  $\mu$ l of EUB 338 FISH probe (GCTGCCTCCCGTAGGAGT) conjugated to Alexa Fluor 594  
345 (Thermofisher) were added to the samples and incubated at 46 °C overnight (18-24 hrs). Fish

346 were washed in 500  $\mu$ l of wash 1 [0.09 M NaCl, 0.02 M Tris pH 7.5, 0.01 % SDS, 20 %  
347 formamide] for 30 mins at 48 °C followed by 1000  $\mu$ l of wash 2 [0.09 M NaCl, 0.02 M Tris pH  
348 7.5, 0.01 % SDS] for 30 mins at 48 °C and resuspended in 500  $\mu$ l of resuspension buffer [0.02  
349 M Tris, 0.01 % SDS] for 30 mins at RT in the dark. For mucus labelling, the resuspension  
350 buffer was replaced by 200  $\mu$ l of 40  $\mu$ g/ml Oregon Green labeled Wheat Germ Agglutinin  
351 (WGA) (Thermofisher) for 25 mins at RT in the dark. The labelling solution was removed, and  
352 samples were further washed twice in resuspension buffer for 5 minutes each. Samples were  
353 incubated in 200  $\mu$ l of 0.55  $\mu$ M DAPI for 10 mins at RT. Samples were washed twice with  
354 resuspension buffer. Samples were mounted on Ultrastick glass slides. Fish were oriented so  
355 larvae will be on its side. Specimens were mounted in Vectashield anti-fade reagent (Vector  
356 Laboratories).

357

### 358 **Zebrafish confocal image acquisition and pre-processing**

359 A Zeiss LSM 710 confocal microscope (Carl Zeiss) was used to acquire spectral images. All  
360 images were acquired with Plan-Apochromat 20x 0.8 NA objective in lambda mode with 29.1  
361 nm channel bandwidth resulting in 9 channels detected over the visible spectrum. Simultaneous  
362 excitation with 405 nm, 488 nm and 561 nm lasers was used. 3-D z-stack images were acquired  
363 as tile scans with 9 z-planes centered in the middle of the gut spanning 8.3  $\mu$ m total in z  
364 dimension. Linear unmixing was performed on the spectrally acquired images after stitching  
365 the tiles together in ZEN software v 3.4. We extracted the reference spectra for DAPI, EUB  
366 338 Alexa flour 594, WGA Oregon green 488 and autofluorescence from the labelled zebrafish  
367 and applied them for the linear unmixing.

368

### 369 **Image quantification and analyses**

370 The unmixed images were further processed and analyzed in IMARIS v 9.6.1 (Bitplane) to  
371 quantify the bacteria biovolume and mucus intensity. For each larva, measurements were made  
372 separately in 3 gastrointestinal regions: the bulb, proximal and distal gut. The bulb region was  
373 defined using visual identification of the pylorus. The remainder of the GI tract, the intestine,  
374 was divided into two equal halves to define the proximal and distal gut in this analysis. For each  
375 of the three manually segmented regions 3D surfaces were generated for the labelled bacteria,  
376 using the default threshold algorithm in IMARIS v. 9.6.1 (Bitplane). After rendering surfaces,  
377 total volume measurements were calculated for bacteria.

378

379 To quantify mucus, the gut was manually segmented in each of the 9 z-planes for each larva  
380 using the columnar epithelium DAPI signal as a guide, because WGA labels both mucus as  
381 well as cell membrane glycoproteins present throughout zebrafish tissues. The WGA channel  
382 for the manually segmented region of interest in the gut lumen. Total intensity of WGA label  
383 in that area in each of the 9 z-planes was measured, then divided by the surface area of the  
384 manually segmented gut region of interest.

385

### 386 **Imaging statistical analyses**

387 Students t-test was used to compare normalized mucus intensity between the conventional and  
388 Mix9 conditions. ANOVA (parametric) with Tukey post hoc test was used to compare  
389 variations in normalized mucus intensity in the intensity for the axenic, Mix9 and conventional  
390 conditions. For the comparison of the total bacteria biovolume. All analyses were done in R  
391 (v4.1.3).

392

### 393 **Histological analysis of zebrafish tissues**

394 Histological sections were used to compare microscopical tissular organization between  
395 Conv, GF and mix9 zebrafish larvae. A total of 5 fish were sacrificed and fixed for 1 day in  
396 Carnoy's fixative. Whole fixed animals were then dehydrated in methanol (2 x 30 minutes)  
397 then in ethanol 100 % (2 x 20 min). Final dehydration was performed by 100 % xylene  
398 solution 2 × 2 hours. Then, samples were embedded in paraffin wax solution (3 x 2 hours) and  
399 embedded in paraffin wax for polymerization. Sections (thickness 5µm) were cut with a  
400 microtome RM2245 (Leica Microsystems GmbH, Wien, Austria), and mounted on adhesive  
401 slides (Klinipath- KP-PRINTER ADHESIVES). Paraffin-embedded sections were  
402 deparaffinized and stained with Alcian Blue (AB) and Periodic-Acid Schiff (PAS) to observe  
403 both neutral and acidic mucins and Goblet cells quantification. All slides were scanned with  
404 the Panoramic Scan 150 (3D Hitech) and analyzed with the CaseCenter 2.9 viewer (3D  
405 Hitech). Goblet cells quantification was estimated by manual counting of total AB positive  
406 cells in blue per villi of the posterior gut.

407

## 408 **Acknowledgements**

409 We are grateful to Bianca Audrain for assistance with obtaining the animal ethical  
410 authorization. Zebrafish embryos were obtained from Sebastian Bedu at the Zoragl'hub  
411 platform at Institut Pasteur. This work was supported by U.S. National Institutes of Health  
412 Grant R01DE030927 to AMV, the French Government's Investissement d'Avenir program,  
413 Laboratoire d'Excellence "Integrative Biology of Emerging Infectious Diseases" (grant  
414 n°ANR-10-LABX-62-IBEID) to JMG, the Fondation pour la Recherche Médicale (grant  
415 DEQ20180339185) to JMG, and a grant from the Philippe Foundation to RJS. Sequencing  
416 was performed by G M. Haustant, L. Lemée, Biomics Platform, C2RT, Institut Pasteur, Paris,  
417 France, supported by France Génomique (ANR-10-INBS-09-09) and IBISA.

418

## 419 **Author Contributions**

420 All authors contributed conception and design of the study. EA performed all microscopy and  
421 image analysis, with assistance from RJS and AMV. RJS and DPP performed the zebrafish  
422 experiments. RJS performed the 16S rRNA gene amplicon study and analyzed the data. JMG  
423 and AMV acquired funding for the study. All authors contributed to manuscript revision, read  
424 and approved the submitted version.

425

## 426 **Ethics Statement**

427 All animal experiments described in the present study were conducted at the Institut Pasteur  
428 according to European Union guidelines for handling of laboratory animals  
429 ([http://ec.europa.eu/environment/chemicals/lab\\_animals/home\\_en.htm](http://ec.europa.eu/environment/chemicals/lab_animals/home_en.htm)) and authorized by the  
430 Institut Pasteur institutional Animal Health and Care Committees under permit #dap200024.

431

## 432 **Conflict of Interest**

433 The authors declare no conflict of interest.

434

## 435 **Data Availability**

436 The raw 16S rRNA gene amplicon sequences generated for this study can be found in the NCBI  
437 Sequencing Read Archive in [BioProject no. PRJNA928247](#). All other raw data, processed

438 sequencing files, and scripts to reproduce the figures in the manuscript are available in the  
439 Zenodo repository, <https://doi.org/10.5281/zenodo.7573109> (47).  
440

## 441 **References**

- 442 1. Hill JH, Round JL. Snapshot: Microbiota effects on host physiology. *Cell*.  
443 2021;184(10):2796-2796.e1.
- 444 2. Obeng N, Bansept F, Sieber M, Traulsen A, Schulenburg H. Evolution of Microbiota–  
445 Host Associations: The Microbe’s Perspective. *Trends in Microbiology*. Elsevier Ltd;  
446 2021. p. 1–9.
- 447 3. Henry LP, Bruijning M, Forsberg SKG, Ayroles JF. The microbiome extends host  
448 evolutionary potential. *Nat Commun*. 2021;12(5141):1–13.
- 449 4. Libertucci J, Young VB. The role of the microbiota in infectious diseases. *Nat Microbiol*.  
450 2019;4(1):35–45.
- 451 5. Wilkins LGE, Leray M, O’Dea A, Yuen B, Peixoto R, Pereira TJ, et al. Host-associated  
452 microbiomes drive structure and function of marine ecosystems. *PLOS Biol*. 2019 Nov  
453 11;17(11):e3000533.
- 454 6. Clavel T, Lagkouvardos I, Stecher B. From complex gut communities to minimal  
455 microbiomes via cultivation. *Curr Opin Microbiol*. 2017;38(June):148–55.
- 456 7. Amato KR, Maurice CF, Guillemin K, Giles-Vernick T. Multidisciplinary in  
457 Microbiome Research: A Challenge and Opportunity to Rethink Causation, Variability,  
458 and Scale. *BioEssays*. 2019;41(10):1–9.
- 459 8. Pollock J, Glendinning L, Wisedchanwet T, Watson M. The Madness of Microbiome:  
460 Attempting To Find Consensus “Best Practice” for 16S Microbiome Studies. *Appl*  
461 *Environ Microbiol*. 2018 Mar 19;84(7):e02627-17.
- 462 9. Eberl C, Ring D, Münch PC, Beutler M, Basic M, Slack EC, et al. Reproducible  
463 Colonization of Germ-Free Mice With the Oligo-Mouse-Microbiota in Different Animal  
464 Facilities. *Front Microbiol*. 2020;10(January):1–15.
- 465 10. Darnaud M, De Vadder F, Bogeat P, Boucinha L, Bulteau AL, Bunescu A, et al. A  
466 standardized gnotobiotic mouse model harboring a minimal 15-member mouse gut  
467 microbiota recapitulates SOPF/SPF phenotypes. *Nat Commun*. 2021 Nov 18;12(1):6686.
- 468 11. Milligan-Myhre K, Charette JR, Phennicie RT, Stephens WZ, Rawls JF, Guillemin K, et  
469 al. Study of Host-Microbe Interactions in Zebrafish. In: *Methods in Cell Biology*.  
470 Academic Press Inc.; 2011. p. 87–116.
- 471 12. Stagaman K, Sharpton TJ, Guillemin K. Zebrafish microbiome studies make waves. *Lab*  
472 *Anim*. 2020 Jun 15;49(7):201–7.
- 473 13. Stressmann FA, Bernal-Bayard J, Perez-Pascual D, Audrain B, Rendueles O, Briolat V, et  
474 al. Mining zebrafish microbiota reveals key community-level resistance against fish  
475 pathogen infection. *ISME J*. 2021;15(3):702–19.

- 476 14. Amann RI, Binder BJ, Olson RJ, Chisholm SW, Devereux R, Stahl DA. Combination of  
477 16S rRNA-targeted oligonucleotide probes with flow cytometry for analyzing mixed  
478 microbial populations. *Appl Environ Microbiol.* 1990 Jun;56(6):1919–25.
- 479 15. Jevtov I, Samuelsson T, Yao G, Amsterdam A, Ribbeck K. Zebrafish as a model to study  
480 live mucus physiology. *Sci Rep.* 2014 Oct 17;4(1):6653.
- 481 16. Donaldson GP, Lee SM, Mazmanian SK. Gut biogeography of the bacterial microbiota.  
482 *Nat Rev Microbiol.* 2016 Jan;14(1):20–32.
- 483 17. Martens EC, Neumann M, Desai MS. Interactions of commensal and pathogenic  
484 microorganisms with the intestinal mucosal barrier. *Nat Rev Microbiol.* 2018  
485 Aug;16(8):457–70.
- 486 18. Hecht AL, Casterline BW, Choi VM, Bubeck Wardenburg J. A Two-Component System  
487 Regulates *Bacteroides fragilis* Toxin to Maintain Intestinal Homeostasis and Prevent  
488 Lethal Disease. *Cell Host Microbe.* 2017 Oct 11;22(4):443-448.e5.
- 489 19. Co JY, Cárcamo-Oyarce G, Billings N, Wheeler KM, Grindy SC, Holten-Andersen N, et  
490 al. Mucins trigger dispersal of *Pseudomonas aeruginosa* biofilms. *Npj Biofilms  
491 Microbiomes.* 2018 Dec;4(1):23.
- 492 20. Mony C, Vandenkoornhuysen P, Bohannan BJM, Peay K, Leibold MA. A Landscape of  
493 Opportunities for Microbial Ecology Research. *Front Microbiol.* 2020 Nov 20;11:561427.
- 494 21. Smith TJ, Sundarraman D, Melancon E, Desban L, Parthasarathy R, Guillemin K. A  
495 mucin-regulated adhesin determines the intestinal biogeography and inflammatory  
496 character of a bacterial symbiont [Internet]. bioRxiv; 2022. Available from:  
497 <https://www.biorxiv.org/content/10.1101/2022.07.25.501442v1>
- 498 22. Tropini C, Earle KA, Huang KC, Sonnenburg JL. The gut microbiome: Connecting  
499 spatial organization to function. *Cell Host Microbe.* 2017 Apr 12;21(4):433–42.
- 500 23. Albenberg L, Esipova TV, Judge CP, Bittinger K, Chen J, Laughlin A, et al. Correlation  
501 between intraluminal oxygen gradient and radial partitioning of intestinal microbiota.  
502 *Gastroenterology.* 2014 Nov;147(5):1055-1063.e8.
- 503 24. Berry D, Stecher B, Schintlmeister A, Reichert J, Brugiroux S, Wild B, et al. Host-  
504 compound foraging by intestinal microbiota revealed by single-cell stable isotope  
505 probing. *Proc Natl Acad Sci U S A.* 2013 Mar 19;110(12):4720–5.
- 506 25. Vaishnava S, Yamamoto M, Severson KM, Ruhn KA, Yu X, Koren O, et al. The  
507 antibacterial lectin RegIII $\gamma$  promotes the spatial segregation of microbiota and host in the  
508 intestine. *Science.* 2011 Oct 14;334(6053):255–8.
- 509 26. O'May GA, Reynolds N, Smith AR, Kennedy A, Macfarlane GT. Effect of pH and  
510 antibiotics on microbial overgrowth in the stomachs and duodena of patients undergoing  
511 percutaneous endoscopic gastrostomy feeding. *J Clin Microbiol.* 2005 Jul;43(7):3059–65.
- 512 27. Jakobsson HE, Rodríguez-Piñero AM, Schütte A, Ermund A, Boysen P, Bemark M, et al.  
513 The composition of the gut microbiota shapes the colon mucus barrier. *EMBO Rep.* 2015  
514 Feb;16(2):164–77.

- 515 28. Johansson MEV, Jakobsson HE, Holmén-Larsson J, Schütte A, Ermund A, Rodríguez-  
516 Piñeiro AM, et al. Normalization of Host Intestinal Mucus Layers Requires Long-Term  
517 Microbial Colonization. *Cell Host Microbe*. 2015 Nov 11;18(5):582–92.
- 518 29. Rodríguez-Piñeiro AM, Johansson MEV. The colonic mucus protection depends on the  
519 microbiota. *Gut Microbes*. 2015 Sep 3;6(5):326–30.
- 520 30. Bates JM, Mittge E, Kuhlman J, Baden KN, Cheesman SE, Guillemin K. Distinct signals  
521 from the microbiota promote different aspects of zebrafish gut differentiation. *Dev Biol*.  
522 2006 Sep 15;297(2):374–86.
- 523 31. Rawls JF, Samuel BS, Gordon JI. Gnotobiotic zebrafish reveal evolutionarily conserved  
524 responses to the gut microbiota. *Proc Natl Acad Sci*. 2004 Mar 30;101(13):4596–601.
- 525 32. Weitekamp CA, Kvasnicka A, Keely SP, Brinkman NE, Howey XM, Gaballah S, et al.  
526 Monoassociation with bacterial isolates reveals the role of colonization, community  
527 complexity and abundance on locomotor behavior in larval zebrafish. *Anim Microbiome*.  
528 2021;3(1).
- 529 33. Afrizal A, Jennings SAV, Hitch TCA, Riedel T, Basic M, Panyot A, et al. Enhanced  
530 cultured diversity of the mouse gut microbiota enables custom-made synthetic  
531 communities. *Cell Host Microbe*. 2022 Nov;30(11):1630-1645.e25.
- 532 34. Rendueles O, Ferrières L, Frétau M, Bégaud E, Herbomel P, Levraud JP, et al. A new  
533 zebrafish model of oro-intestinal pathogen colonization reveals a key role for adhesion in  
534 protection by probiotic bacteria. *PLoS Pathog*. 2012 Jul;8(7):12.
- 535 35. Eren AM, Vineis JH, Morrison HG, Sogin ML. A Filtering Method to Generate High  
536 Quality Short Reads Using Illumina Paired-End Technology. *PLoS ONE*.  
537 2013;8(6):e66643.
- 538 36. Huse SM, Mark Welch DB, Voorhis A, Shipunova A, Morrison HG, Eren AM, et al.  
539 VAMPS: A website for visualization and analysis of microbial population structures.  
540 *BMC Bioinformatics*. 2014 Feb 5;15(1):41.
- 541 37. Callahan BJ, McMurdie PJ, Rosen MJ, Han AW, Johnson AJA, Holmes SP. DADA2:  
542 High-resolution sample inference from Illumina amplicon data. *Nat Methods*. 2016 Jul  
543 23;13(7):581–3.
- 544 38. Caporaso JG, Kuczynski J, Stombaugh J, Bittinger K, Bushman FD, Costello EK, et al.  
545 QIIME allows analysis of high-throughput community sequencing data. Vol. 7, *Nature*  
546 *Methods*. 2010. p. 335–6.
- 547 39. Bokulich NA, Kaehler BD, Rideout JR, Dillon M, Bolyen E, Knight R, et al. Optimizing  
548 taxonomic classification of marker-gene amplicon sequences with QIIME 2's q2-feature-  
549 classifier plugin. *Microbiome*. 2018 Dec 17;6(1):90.
- 550 40. Bolyen E, Rideout JR, Dillon MR, Bokulich NA, Abnet CC, Al-Ghalith GA, et al.  
551 Reproducible, interactive, scalable and extensible microbiome data science using QIIME  
552 2. *Nat Biotechnol*. 2019 Jul 24;37(8):852–7.

- 553 41. Reitmeier S, Hitch TCA, Treichel N, Fikas N, Hausmann B, Ramer-Tait AE, et al.  
554 Handling of spurious sequences affects the outcome of high-throughput 16S rRNA gene  
555 amplicon profiling. *ISME Commun.* 2021 Jun 29;1(1):31.
- 556 42. Dixon P. VEGAN, a package of R functions for community ecology. *J Veg Sci.* 2003 Dec  
557 1;14(6):927–30.
- 558 43. McMurdie PJ, Holmes S. Phyloseq: An R Package for Reproducible Interactive Analysis  
559 and Graphics of Microbiome Census Data. Watson M, editor. *PLoS ONE.* 2013 Apr  
560 22;8(4):e61217.
- 561 44. Wickham H, Averick M, Bryan J, Chang W, McGowan L, François R, et al. Welcome to  
562 the Tidyverse. *J Open Source Softw.* 2019;4(43):1686.
- 563 45. Warton DI, Wright ST, Wang Y. Distance-based multivariate analyses confound location  
564 and dispersion effects. *Methods Ecol Evol.* 2012 Feb 1;3(1):89–101.
- 565 46. McArdle BH, Anderson MJ. FITTING MULTIVARIATE MODELS TO COMMUNITY  
566 DATA: A COMMENT ON DISTANCE-BASED REDUNDANCY ANALYSIS.  
567 *Ecology.* 2001 Jan;82(1):290–7.
- 568 47. Stevick R, Adade EE. Analyses for Gnotobiotic zebrafish microbiota display inter-  
569 individual variability affecting host physiology. Zenodo.  
570 2023;<https://doi.org/10.5281/zenodo.7573109>.
- 571